

---

---

# [<sup>18</sup>F]FET PET/MRI: An Accurate Technique for Detection of Small Functional Pituitary Tumors

Ilanah J. Pruis<sup>1</sup>, Frederik A. Verburg<sup>1</sup>, Rutger K. Balvers<sup>2</sup>, Anita A. Hartevelde<sup>1</sup>, Richard A. Feelders<sup>3</sup>, Meike W. Vernooij<sup>1,4</sup>, Marion Smits<sup>1,5</sup>, Sebastian J.C.M.M. Neggers<sup>\*3</sup>, and Sophie E.M. Veldhuijzen van Zanten<sup>\*1</sup>

<sup>1</sup>Department of Radiology and Nuclear Medicine, Erasmus MC, Rotterdam, The Netherlands; <sup>2</sup>Department of Neurosurgery, Erasmus MC, Rotterdam, The Netherlands; <sup>3</sup>Department of Medicine, Section of Endocrinology, Erasmus MC, Rotterdam, The Netherlands; <sup>4</sup>Department of Epidemiology, Erasmus MC, Rotterdam, The Netherlands; and <sup>5</sup>Medical Delta, Delft, The Netherlands

---

Small functional pituitary tumors can cause severely disabling symptoms and early death. The gold standard diagnostic approach includes laboratory tests and MRI, with or without inferior petrosal sinus sampling (IPSS). In up to 40% of patients, however, the source of excess hormone production remains unidentified or uncertain. This excludes patients from surgical, Gamma Knife, and CyberKnife therapy and adversely affects overall cure rates. We here assess the diagnostic yield of O-(2-[<sup>18</sup>F]fluoroethyl)-L-tyrosine ([<sup>18</sup>F]FET) PET/MRI for detection of small functional pituitary tumors in these patients.

**Methods:** This retrospective analysis included patients with Cushing disease (CD) but prior negative or inconclusive MRI results who underwent [<sup>18</sup>F]FET PET/MRI between February 1, 2021, and December 1, 2022. PET/MR images and MR images alone were evaluated by experienced nuclear radiologists, neuroradiologists, or radiologists. Post-operative tissue analysis (when performed) was used as a reference standard to assess diagnostic metrics (i.e., sensitivity and positive predictive value). Results were also compared with previously obtained MR images, preceding IPSS, and clinical or biochemical follow-up. **Results:** Twenty-two patients (68% female; mean age ± SD, 48 ± 15y; range, 24–68y) were scanned. All patients showed a clear metabolic focus on [<sup>18</sup>F]FET PET, whereas reading of the MRI alone yielded a suspected lesion in only 50%. Fifteen patients underwent surgery directed at the [<sup>18</sup>F]FET-positive focus. Tissue analysis confirmed a pituitary adenoma/pituitary neuroendocrine tumor of the corticotroph cell type (TPIT lineage) in 10 of 15 and a pituitary tumor in 1 of 15, rendering a sensitivity of 100% and a positive predictive value of 73%. Lateralization was more accurate with [<sup>18</sup>F]FET PET/MRI than with IPSS in 33%. Twelve of 16 (75%) patients who received surgical, Gamma Knife, or CyberKnife therapy after [<sup>18</sup>F]FET PET/MRI reached short-term remission. **Conclusion:** [<sup>18</sup>F]FET PET/MRI shows a high diagnostic yield for localizing small functional pituitary tumors. This multimodal imaging technique provides a welcome improvement for diagnosis, planning of surgery, and clinical outcome in patients with Cushing disease, particularly those with repeated negative or inconclusive MRI results with or without IPSS.

**Key Words:** Cushing disease; pituitary tumor; [<sup>18</sup>F]FET; PET/MRI

J Nucl Med 2024; 65:688–692

DOI: 10.2967/jnumed.123.266853

**S**mall functional pituitary tumors can cause severely disabling symptoms and early death due to autonomous excess production of hormones such as adrenocorticotropic hormone (ACTH), resulting in Cushing disease (CD) (1).

In up to 40% of patients, conventional diagnostic MRI is inconclusive, as the lesions by definition are smaller than 10 mm in diameter and not always sufficiently contrasting with normal pituitary tissue after the administration of a gadolinium-based contrast agent (2,3). Even advanced MRI techniques, such as dynamic perfusion imaging, can leave small lesions undetected in up to one third of patients (2–4). When MRI suggests a possible tumor no more than 6 mm in diameter, the current diagnostic guideline (5) recommends additional inferior petrosal sinus sampling (IPSS) to confirm and possibly lateralize the potential source of excess hormone production. IPSS, however, is an invasive procedure and a derivative way to lateralize or localize a lesion, which does not accurately guide ever-improving precision surgery. According to the literature, a positive preoperative MRI result (i.e., accurate localization) is generally associated with a higher cure rate (i.e., remission) after surgery (6). This goes along with adequate experience of the neurosurgeon, which also has been shown to be an important determinant of outcome (7). Patients with nonvisible lesions usually undergo multiple diagnostic procedures over several months' time, undergo more extensive exploration during surgery, and generally show lower cure rates (8), rendering evident the high unmet need for improved diagnostic techniques to accurately localize small functional pituitary tumors.

PET of the pituitary has been evaluated in several cohort studies and small clinical series using various tracers (9,10). Results with regard to their diagnostic value vary widely for the detection of small pituitary tumors. [<sup>18</sup>F]FDG and [<sup>68</sup>Ga]Ga-DOTATATE/TOC, for example, show highly variable physiologic uptake in the pituitary hampering lesion detection. The amino acid tracer L-[methyl-<sup>11</sup>C]-methionine showed promising results but can also suffer from high physiologic uptake in the pituitary and has a short half-life (11). The amino acid tracer O-(2-[<sup>18</sup>F]fluoroethyl)-L-tyrosine ([<sup>18</sup>F]FET) could potentially aid and improve the detection of small functional tumors, as was also indicated by 2 case reports (12,13) and a first exploratory series of 9 patients with CD (14). In addition, preclinical research showed that the main target for [<sup>18</sup>F]FET, human system L amino acid transporter, is overexpressed in pituitary adenoma/pituitary neuroendocrine tumor (PitNET) (15,16), formerly known as pituitary adenoma, in contrast to normal pituitary cells (17). The primary aim of this study was to assess the clinical diagnostic yield of [<sup>18</sup>F]FET PET/MRI for localizing small

---

Received Oct. 12, 2023; revision accepted Feb. 13, 2024.  
For correspondence or reprints, contact Sophie E.M. Veldhuijzen van Zanten (s.veldhuijzenvanzanten@erasmusmc.nl).  
<sup>\*</sup>Contributed equally to this work.  
Published online Mar. 21, 2024.  
COPYRIGHT © 2024 by the Society of Nuclear Medicine and Molecular Imaging.

functional pituitary tumors in patients with CD and to determine the sensitivity and positive predictive value (PPV) using postoperative tissue analysis as a reference standard. The secondary aim was to evaluate the results in light of previously obtained MRI, preceding IPSS, and clinical or biochemical follow-up.

## MATERIALS AND METHODS

### Patients

This retrospective study was performed in accordance with the Declaration of Helsinki. The institutional review board of Erasmus Medical Center approved the study, and all patients provided written informed consent for use of imaging and relevant clinical or biochemical data for research purposes. Patients were included if they were 18 y of age or older, presented with clinical signs and symptoms of CD and had biochemically proven CD (primary or recurrent), and had negative and inconclusive results on prior MRI. The enrollment period was February 1, 2021, to December 1, 2022.

### Image Acquisition

Previous MRI was performed within routine clinical care and acquired at either 1.5 or 3 T according to a standard sellar imaging protocol (18). This protocol included coronal T1- and T2-weighted fast spin-echo sequences and a coronal and sagittal T1-weighted fast spin-echo sequence directly after administration of a gadolinium-based contrast agent, all with a voxel size of  $0.3 \times 0.3 \times 3$  mm. ProHance (gadoteridol, 1 mmol/mL; Bracco Diagnostics Inc.) was used as the gadolinium-based contrast agent and administered as a single-dose contrast bolus of 0.2 mL/kg (with a maximum of 15 mL for weights of  $>75$  kg).

$^{18}\text{F}$ FET was purchased commercially from the BV Cyclotron VU. Scans were acquired after a minimum fasting period of 4 h on a Signa PET/MRI 3.0-T scanner (GE Healthcare) at  $\pm 20$  min (range, 19–28 min) after an intravenous injection of  $^{18}\text{F}$ FET (median, 201 MBq; range, 50–207 MBq). A single-bed-position PET acquisition of 20 min was obtained of the brain. Standard 4-tissue (air, lung, water, and fat) MRI Dixon-based attenuation maps were acquired simultaneously, and a standard MRI zero-echo-time scan was acquired that adds bone tissue for the head (19). PET images were reconstructed using the manufacturer's proprietary block-sequential regularized expectation maximization algorithm using time-of-flight information, point-spread function, and a  $\beta$ -value of 300. Attenuation, scatter, and random corrections were applied.

Simultaneously obtained MRI series were acquired according to the standard sellar protocol, to allow for comparison with the yield of previously obtained MRI. T1- and T2-weighted sequences were used for attenuation correction. Postcontrast T1-weighted sequences were obtained directly after the PET acquisition.

### Image Analysis

Scans were visually assessed by an expert nuclear radiologist or nuclear medicine physician using standard clinical software (Vue PACS; Carestream Health, Inc.). Focal uptake visually exceeding local background activity (i.e., surrounding supposed healthy pituitary tissue and brain parenchyma) was considered positive for the presence of a small functional tumor. Additionally, semiquantitative analyses were performed, for which full methods can be found in the supplemental materials (19).

Simultaneously obtained MR images were used for anatomic localization and possible identification of accompanying anatomic changes in pituitary tissue. An independent masked evaluation of the simultaneously obtained MR images (MRI alone) was performed by an expert neuroradiologist. As diagnostic metrics, the sensitivity and PPV were calculated, using postoperative tissue analysis as the reference standard.

## Clinical Parameters

Clinical parameters were derived from the patients' electronic health records and were used for baseline characterization of the total cohort. These parameters comprised age; sex; diagnosis (primary or recurrent CD); results from previous diagnostic tests (i.e., previously obtained MRI and IPSS); total number of previous diagnostic tests (MRI and IPSS); diagnostic interval (in months), defined as time between most recent MRI and  $^{18}\text{F}$ FET PET/MRI; and total diagnostic period (in months), defined as time between first MRI and  $^{18}\text{F}$ FET PET/MRI.

Also, the following information was obtained for each patient: the neurosurgeon's perioperative confirmation that the pituitary tumor was located at the site of uptake on  $^{18}\text{F}$ FET PET/MRI; the results of postoperative pathologic tissue analysis (presence or absence of functional [i.e., hormone-producing] tumor, based on routine immunohistochemistry stainings (15)); the deployed treatment after  $^{18}\text{F}$ FET PET/MRI, such as commencement of medication or performance of surgical, Gamma Knife (Elekta Instruments, Inc.), or CyberKnife (Accuray) therapy (including how many and type of procedure); and the results of clinical or biochemical follow-up to assess potential responses (i.e., remission rates).

For CD, morning plasma cortisol levels were used to determine the immediate postoperative biochemical remission status, in which remission was defined as cortisol levels of less than 50 nmol/L. Sustained biochemical remission was assessed and defined by 24-h urinary free cortisol concentrations ( $<133$  nmol/24 h), midnight salivary cortisol levels ( $<2.8$  nmol/L), and resolution of clinical symptoms (5,20). The first postoperative measurement of cortisol was used in patients who underwent surgery. Liquid chromatography tandem mass spectrometry (Xevo TQ-S; Waters) was used to assess serum, saliva, and urine samples. The upper limit of normal of this assay is 133 nmol/24 h.

## Statistical Analysis

Statistical analysis was performed with Statistical Package for the Social Sciences, version 24.0.0.1 (IBM Corp.).

Normality of the data was determined using Kolmogorov–Smirnov  $z$  scores for continuous variables and was reported by mean  $\pm$  SD for normally distributed variables and by median and interquartile range (IQR) for nonnormally distributed variables. For categorical variables, frequencies and percentages were reported. Patients with and without an available tissue analysis report were compared using the available baseline characteristics. The independent  $t$  test and Mann–Whitney  $U$  test were used for normally and nonnormally distributed variables, respectively. For categorical data, the  $\chi^2$  test was used, and the Fisher exact test was reported instead when the minimum count in a variable was less than 5.  $P$  values of less than 0.05 were considered a statistically significant difference.

## RESULTS

### Patients

Twenty-two patients with CD were included in the study (Supplemental Tables 1 and 2). Mean age was  $48 \pm 15$  y (range, 24–68 y). Most patients were female ( $n = 15$ , 68%). None of the patients used somatostatin analogs during the  $^{18}\text{F}$ FET PET/MRI examination. All patients had undergone one or more preceding MRI scans (median, 1; range, 1–5) at 1.5 T ( $n = 12$ ) or 3.0 T ( $n = 10$ ). The median diagnostic interval was 3.9 mo (IQR, 1.8–5.2 mo), and the median total diagnostic period was 4.9 mo (IQR, 3.7–16.0 mo). For patients with a suspected recurrent small functional tumor, the median interval between the last surgery and  $^{18}\text{F}$ FET PET/MRI was 65.6 mo (IQR, 58.1–159.0 mo), which is beyond the minimal diagnostic interval of 3 mo suggested in guidelines to prevent mistaking postoperative surgical changes for remnant or recurrent lesions (21).

### Clinical Performance of [<sup>18</sup>F]FET PET/MRI for CD

All patients had a positive [<sup>18</sup>F]FET PET/MRI result (Supplemental Table 3; Supplemental Fig. 1) as determined by both readers, without discrepancies. The results of semiquantitative analyses are shown in Supplemental Tables 4 and 5. Independent scoring of the MRI alone showed an identifiable lesion in 11 of 22 (50%).

After [<sup>18</sup>F]FET PET/MRI, 1 patient (patient 14) underwent Gamma Knife therapy, and 15 of 22 patients (68%) underwent transsphenoidal surgery. The neurosurgeon confirmed that tumor tissue was found at the location of [<sup>18</sup>F]FET uptake in 15 of 15 patients (100%). Postoperative tissue analysis was positive for functional tumor tissue in 11 of 15 patients (73%). In 10 of 15 patients, immunohistochemistry confirmed resection of a pituitary adenoma/PitNET of the corticotroph cell type (i.e., the transcription factor of the functioning corticotroph adenoma [TPIT] lineage), formerly reported as ACTH-producing adenoma (one of which is exemplified in Fig. 1), and in 1 patient (patient 20) a pituicytoma was resected (Fig. 2). One of the patients (patient 16) underwent repeated postoperative PET/MRI showing no residual uptake of [<sup>18</sup>F]FET (Fig. 3). In 4 of 15 patients who underwent surgery, there was not enough material for the pathologist to make a correct diagnosis (Supplemental Table 3). Hence, the sensitivity of [<sup>18</sup>F]FET PET/MRI in our cohort was 100% and PPV 73%.

With a median postsurgical ( $n = 15$ ) or Gamma Knife ( $n = 1$ ) follow-up period of 10 mo (IQR, 4–16 mo), biochemical remission was observed in 12 of 16 patients (75%), who included all 4 patients with inconclusive tissue analysis (patients 4, 6, 9, and 17). One of these patients (patient 4) initially did not show biochemical remission; a repeated postoperative [<sup>18</sup>F]FET PET/MRI was performed that showed unchanged focal uptake. After second-look surgery, although tissue analysis was again inconclusive, this patient reached biochemical remission. Of the 4 of 16 patients who had not reached biochemical remission at the time this article was being prepared, 1 patient (patient 5) underwent repeated postoperative [<sup>18</sup>F]FET PET/MRI showing unchanged focal uptake in 1 of the 2 lesions that were preoperatively identified. This patient is currently awaiting second-look surgery (Supplemental Table 3). Patient 18 remained with mild postoperative symptoms and biochemical abnormalities fitting active CD, despite the fact that postoperative tissue analysis reported the presence of pituitary adenoma/PitNET. The neurosurgeon retrospectively confirmed that not all tissue could be removed because it was near vital structures (e.g., the carotid artery). This patient is scheduled for CyberKnife therapy. Patient 20, with postoperatively confirmed pituicytoma, also remained symptomatic (Fig. 2). This patient is scheduled for repeated [<sup>18</sup>F]FET PET/MRI to evaluate the need for second-look surgery. The patient who underwent Gamma

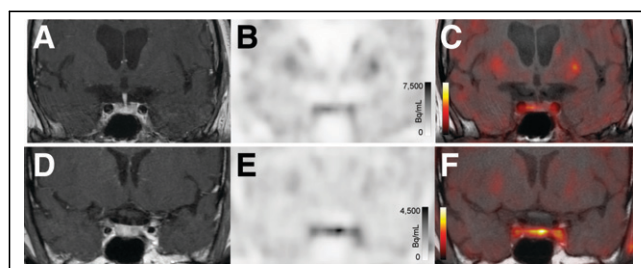


**FIGURE 1.** Coronal T1-weighted postgadolinium MR (A and D), [<sup>18</sup>F]FET PET (B and E), and PET/MR (C and F) images centered at pituitary of patients 11 (A–C) and 12 (D–F), showing clear focal uptake that could be differentiated from uptake in rest of pituitary tissue. Postoperative tissue analysis reported resection of small pituitary adenoma/PitNET.



**FIGURE 2.** Coronal T1-weighted postgadolinium MR (A), [<sup>18</sup>F]FET PET (B), and PET/MR (C) images centered at pituitary of patient 20, showing clear focal uptake. Postoperative tissue analysis reported pituicytoma.

Knife therapy (patient 14) did not yet show biochemical remission after 9 mo of follow-up, a finding that is not surprising given that 12–60 mo are usually needed for this treatment to take effect (22).

Six (of 22) patients (27%) did not undergo surgery, Gamma Knife, or CyberKnife therapy. These patients did not differ from the other patients with regard to age ( $P = 0.44$ ), sex ( $P = 1.00$ ), and a primary or recurrent diagnosis ( $P = 1.00$ ). Four are currently under medical pretreatment while awaiting surgery, one (patient 10) refused surgery and is medically controlled by cabergoline, and one (patient 8) died from another medical condition.

### Added Value of [<sup>18</sup>F]FET PET/MRI

[<sup>18</sup>F]FET PET/MRI was particularly useful in 1 (patient 16) of the 11 patients who had a tumor as confirmed by the neurosurgeon and by postoperative tissue analysis, with PET showing focal uptake of [<sup>18</sup>F]FET whereas no lesion could be delineated on previously obtained MRI (diagnostic interval, 9 mo). And in 1 patient (patient 5), 2 lesions were identified by [<sup>18</sup>F]FET PET whereas no lesion was identified on masked reading of the simultaneous MRI alone and only 1 lesion had been suspected on the previously obtained MRI (diagnostic interval, 5 mo). In the other 9 of 11 patients (82%), [<sup>18</sup>F]FET PET/MRI confirmed the location of a lesion that had been suspected but uncertain on previously obtained MRI (totaling between 1 and 5 per patient; median diagnostic interval, 4 mo; total diagnostic period, 5 mo).

All 17 patients with primary CD had also undergone IPSS confirming central ACTH production. On [<sup>18</sup>F]FET PET/MRI, 12 of 17 underwent surgery, 9 of whom had a functional tumor confirmed by the neurosurgeon and postoperative tissue analysis. [<sup>18</sup>F]FET PET/MRI was particularly useful in 2 of 9 patients (22%) for whom IPSS could not differentiate between a left and right localization. In 1 patient (11%), lateralization based on IPSS

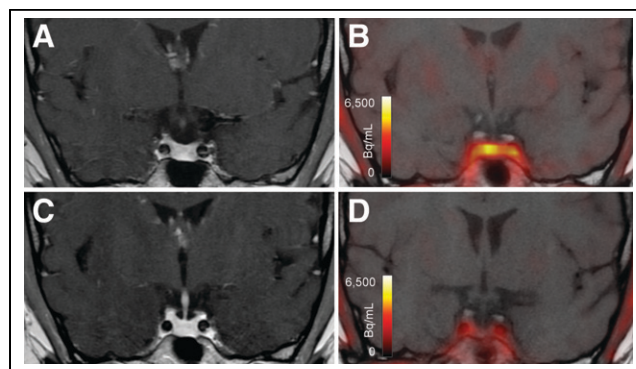


**FIGURE 3.** T1-weighted postgadolinium MR image (A and C) and [<sup>18</sup>F]FET PET/MR image (B and D) centered at pituitary before (A and B) and after (C and D) transsphenoidal surgery. This patient with CD (patient 16) showed clear focal uptake (B) but no clear lesion on previously obtained and accompanying MRI (A). Postoperative tissue analysis did confirm resection of small pituitary adenoma/PitNET, and postoperative [<sup>18</sup>F]FET PET showed no residual uptake (D).

did not correspond with the actual location of the lesion as identified on [<sup>18</sup>F]FET PET/MRI and confirmed by the neurosurgeon and tissue analysis. In 6 of 9 patients (67%), lateralization based on IPSS corresponded with the location of the lesion as identified on [<sup>18</sup>F]FET PET/MRI.

## DISCUSSION

In this study, we investigated the clinical diagnostic yield of the novel multimodal imaging technique [<sup>18</sup>F]FET PET/MRI in patients with clinical symptoms of CD but negative or inconclusive results from standard diagnostic approaches (i.e., MRI alone with or without IPSS) as recommended by the reigning guideline (5). [<sup>18</sup>F]FET PET/MRI showed a high yield (sensitivity, 100%; PPV, 73%) and accurate localization of small functional pituitary tumors. Resulting from this novel diagnostic approach, 16 of 22 patients received treatment directed at an identified [<sup>18</sup>F]FET-positive focus. Success rates after surgical, Gamma Knife, or CyberKnife therapies were deemed high, reflected by short-term remission in 12 of 16 (75%) patients.

Calculations for sensitivity and PPV were based on postoperative tissue analysis as the reference standard. Some patients with positive tissue analysis, however, did not show clinical remission, whereas some patients with negative tissue analysis did. We hypothesize that the former is the result of residual tumor (confirmed in 1 patient by repeated [<sup>18</sup>F]FET PET/MRI), for which these patients are awaiting second-look surgery ( $n = 2$ ) or CyberKnife therapy ( $n = 1$ ). Clinical remission with negative tissue analysis, on the other hand, is likely the result of sampling bias since the neurosurgeon did confirm the presence of adenoma tissue at the location of [<sup>18</sup>F]FET uptake on PET images for these patients. Other measures of performance (specificity, NPV, and accuracy) could not be determined because none of the patients in our cohort had negative scan findings, necessitating further research with larger patient numbers. Nonetheless, it will remain challenging to determine specificity, NPV, and accuracy using a tissue analysis–based reference (unless an ectopic source of excess hormone production is detected), since transphenoidal surgery or biopsy is not desired in a patient with a negative scan result. These 2 points show the need to evaluate a more holistic reference standard in future advanced imaging studies.

Additional to high sensitivity and high PPV, we found particular value in the possibility to define the exact location (i.e., left or right) of the pituitary tumor, which was better for [<sup>18</sup>F]FET PET/MRI than for IPSS. IPSS has a reported sensitivity of about 94% and PPV of about 89% to detect a central (i.e., pituitary) versus an ectopic ACTH-producing source (23,24) but was never validated for the assessment of lateralization (5). In our cohort, the exact localization of a small functional tumor could accurately be indicated on [<sup>18</sup>F]FET PET/MRI. This is of great clinical value because it allows precision surgery and targeted Gamma Knife or CyberKnife therapy. The latter has been shown to be a valuable adjuvant when surgery or medical treatment is not available, fails, or is poorly tolerated (22), as exemplified by patient 18, with parasellar extension. Our results suggest that, besides having value for diagnosis and treatment planning, [<sup>18</sup>F]FET PET/MRI could offer a remarkable time gain and a lower patient burden, which may also reduce burden and costs for the health-care system as a whole.

[<sup>18</sup>F]FET is not well known yet for detecting small functional pituitary tumors but is increasingly applied for gliomas (25) and therefore is becoming more widely available. [<sup>18</sup>F]FET also

compares favorably in biodistribution to other tracers that have been evaluated for the detection of pituitary tumors in CD (10), such as [<sup>18</sup>F]FDG and somatostatin- or corticotrophic receptor–targeting tracers ([<sup>68</sup>Ga]Ga-DOTATATE/TOC and [<sup>68</sup>Ga]Ga-DOTA-CRH). Compared with the most favorable amino acid tracer, L-[methyl-<sup>11</sup>C]-methionine, [<sup>18</sup>F]FET has a more practical half-life (110 vs. 20 min) and shows much less background uptake in the pituitary (26). The latter improves the yield, particularly for detection and delineation of small lesions, which are relatively common in patients with CD (3,27). Other tracers, such as [<sup>18</sup>F]F-DOPA and [<sup>18</sup>F]F-fallypride, have also been reported for detection of pituitary tumor but not specifically for patients with CD (9).

To date, 1 retrospective study has been published in which PET/MRI with [<sup>18</sup>F]FET ( $n = 6$ ), L-[methyl-<sup>11</sup>C]-methionine ( $n = 6$ ), or both in a serial manner ( $n = 3$ ) was applied in patients with CD (14). A sensitivity and PPV of 100% were reported for localization of a small functional pituitary adenoma/PitNET using [<sup>18</sup>F]FET PET/MRI (14); however, only patients with a postoperatively confirmed corticotroph adenoma were included. Our study included patients on the basis of a biochemical diagnosis of CD, whereas repeated MRI scans with or without IPSS showed negative, uncertain, or inconclusive results—representative of frequently observed challenges in daily clinical practice. This provides additional proof of the important added value of [<sup>18</sup>F]FET PET/MRI for patients clinically or biochemically suspected of having a small functional pituitary tumor. We found that [<sup>18</sup>F]FET PET/MRI can detect both pituitary adenoma/PitNETs of the corticotroph cell type (TPIT lineage) and pituicytomas, which are also known to potentially be ACTH-producing (28,29).

In terms of spatial resolution, MRI generally suffices for detection of subtle anatomic disturbances caused by pituitary tumors, with 3 T being favorable over 1.5 T (2,30). In our cohort, the field strength of the previously obtained MRI scans varied, reflective of current clinical practice. A confounder analysis showed no difference in lesions detection rates at 3 T compared with 1.5 T on these prior scans. [<sup>18</sup>F]FET images were obtained on a next-generation 3.0-T PET/MRI scanner, which allowed detection of lesions as small as 3–4 mm, as shown earlier in a pediatric patient (13). Nevertheless, only 50% of lesions were detected when the simultaneously obtained MR images were reviewed separately from the PET images by an expert neuroradiologist. This detection rate improved to 100% when the scans were reviewed in a hybrid manner. Future studies will be directed at head-to-head comparisons of the performance of [<sup>18</sup>F]FET PET and other diagnostic techniques, including advanced MRI sequences such as spoiled gradient-echo 3-dimensional T1-weighted or dynamic perfusion imaging (4), preferably in patients at the time of initial clinical presentation, to determine the place of [<sup>18</sup>F]FET PET in future guidelines.

Our analysis included only patients with CD because of the relatively small number of other diagnoses (i.e., 6 cases of acromegaly and 1 of hyperthyroidism). Evaluation of [<sup>18</sup>F]FET PET/MRI performance for pituitary adenoma/PitNET of other cell types demands further research. Also, the effects of simultaneous use of cabergoline, somatostatin analogs, or steroidogenesis inhibitors on [<sup>18</sup>F]FET uptake should still be investigated (31). Given the relatively small number of patients in this study and the uncontrolled conditions (i.e., real-time clinical practice, with wide variability in preceding or concurrent medicinal treatments), the resulting thresholds from semiquantitative analyses require validation. Future studies should particularly focus on specificity and interobserver variability, such as by masked reading of a mixed cohort of patients

suspected of having a pituitary adenoma/PitNET and patients with supposed healthy pituitary tissue.

## CONCLUSION

[<sup>18</sup>F]FET PET/MRI can detect small pituitary tumors even when MRI alone or previously obtained MRI with or without IPSS does not show a definite lesion. Future randomized controlled studies should be aimed at head-to-head comparisons between PET/MRI using [<sup>18</sup>F]FET, PET/MRI using other amino acid tracers (e.g., L-[methyl-<sup>11</sup>C]-methionine), and MRI alone (with or without addition of PET/CT), with or without IPSS, to assess its diagnostic performance upfront, in terms of not only sensitivity but also specificity. Given further study, it is conceivable that [<sup>18</sup>F]FET PET/MRI might become the diagnostic method of choice (over IPSS) for the identification of an organic correlate of excessive hormone production in the pituitary gland, should MRI alone not provide a sufficient answer and given the availability of the tracer and a hybrid scanner.

## DISCLOSURE

Ilanah Pruis and Sophie Veldhuijzen van Zanten were financially supported by the Semmy Foundation (Stichting Semmy). Marion Smits received speaker honoraria (paid to employer) from AuntMinnie and GE Healthcare and consultancy fees (paid to institution) from Bracco. Frederik Verburg received speaker honoraria (paid to employer) from Sanofi, AstraZeneca, and Bayer and is a consultant to GE Healthcare (paid to employer). No other potential conflict of interest relevant to this article was reported.

## KEY POINTS

**QUESTION:** What is the diagnostic yield of [<sup>18</sup>F]FET PET/MRI for detection of small functional pituitary tumors?

**PERTINENT FINDINGS:** In a convenience series of 22 patients with biochemically proven CD but prior negative or inconclusive MRI results, [<sup>18</sup>F]FET PET/MRI was positive in 100% of patients and showed superior diagnostic performance (sensitivity, 100%; PPV, 73%) to standard modalities for diagnosing small functional tumors. This, in our cohort, led to the initiation of surgical, Gamma Knife, or CyberKnife therapy in 73% of patients, with a high short-term remission rate of 75%.

**IMPLICATIONS FOR PATIENT CARE:** [<sup>18</sup>F]FET PET/MRI is a promising diagnostic technique for the identification of an organic correlate of excessive hormone production in addition to anatomic disturbances in the pituitary gland caused by small functional tumors.

## REFERENCES

1. Molitch ME. Diagnosis and treatment of pituitary adenomas: a review. *JAMA*. 2017;317:516–524.
2. Bonneville JF, Bonneville F, Cattin F. Magnetic resonance imaging of pituitary adenomas. *Eur Radiol*. 2005;15:543–548.
3. Jagannathan J, Sheehan JP, Jane JA Jr. Evaluation and management of Cushing syndrome in cases of negative sellar magnetic resonance imaging. *Neurosurg Focus*. 2007;23:E3.
4. Grober Y, Grober H, Wintermark M, Jane JA, Oldfield EH. Comparison of MRI techniques for detecting microadenomas in Cushing's disease. *J Neurosurg*. 2018;128:1051–1057.
5. Fleseriu M, Auchus R, Bancos I, et al. Consensus on diagnosis and management of Cushing's disease: a guideline update. *Lancet Diabetes Endocrinol*. 2021;9:847–875.
6. Ciric I, Zhao JC, Du H, et al. Transsphenoidal surgery for Cushing disease: experience with 136 patients. *Neurosurgery*. 2012;70:70–80.
7. Shirvani M, Motiei-Langroudi R, Sadeghian H. Outcome of microscopic transsphenoidal surgery in Cushing disease: a case series of 96 patients. *World Neurosurg*. 2016;87:170–175.
8. Hofmann BM, Hlavac M, Martinez R, Buchfelder M, Müller OA, Fahlbusch R. Long-term results after microsurgery for Cushing disease: experience with 426 primary operations over 35 years. *J Neurosurg*. 2008;108:9–18.
9. Gillett D, MacFarlane J, Bashari W, et al. Molecular imaging of pituitary tumors. *Semin Nucl Med*. 2023;53:530–538.
10. Bauman MMJ, Graves JP, Harrison DJ, et al. The utility of PET for detecting corticotropinomas in Cushing disease: a scoping review. *Neurosurg Rev*. 2023;46:160.
11. Bakker LEH, Versteegen MJT, Gharqi E, et al. Implementation of functional imaging using <sup>11</sup>C-methionine PET-CT co-registered with MRI for advanced surgical planning and decision making in prolactinoma surgery. *Pituitary*. 2022;25:587–601.
12. Currie GM, Trifunovic M, Kiat H, et al. Pituitary incidentaloma found on O-(2-<sup>18</sup>F-fluoroethyl)-L-tyrosine PET. *J Nucl Med Technol*. 2014;42:218–222.
13. Veldhuijzen van Zanten SEM, Neggers S, Valkema R, Verburg FA. Positive [<sup>18</sup>F]fluoroethyltyrosine PET/MRI in suspected recurrence of growth hormone-producing pituitary adenoma in a paediatric patient. *Eur J Nucl Med Mol Imaging*. 2021;49:410–411.
14. Berkman S, Roethlisberger M, Mueller B, et al. Selective resection of Cushing microadenoma guided by preoperative hybrid 18-fluoroethyl-L-tyrosine and 11-C-methionine PET/MRI. *Pituitary*. 2021;24:878–886.
15. Asa SL, Mete O, Perry A, Osamura RY. Overview of the 2022 WHO classification of pituitary tumors. *Endocr Pathol*. 2022;33:6–26.
16. Louis DN, Perry A, Wesseling P, et al. The 2021 WHO classification of tumors of the central nervous system: a summary. *Neuro Oncol*. 2021;23:1231–1251.
17. Satou M, Wang J, Nakano-Tateno T, et al. L-type amino acid transporter 1, LAT1, in growth hormone-producing pituitary tumor cells. *Mol Cell Endocrinol*. 2020;515:110868.
18. Gadelha MR, Barbosa MA, Lamback EB, Wildemberg LE, Kasuki L, Ventura N. Pituitary MRI standard and advanced sequences: role in the diagnosis and characterization of pituitary adenomas. *J Clin Endocrinol Metab*. 2022;107:1431–1440.
19. Law I, Albert NL, Arbizu J, et al. Joint EANM/EANO/RANO practice guidelines/SNMMI procedure standards for imaging of gliomas using PET with radiolabelled amino acids and [<sup>18</sup>F]FDG: version 1.0. *Eur J Nucl Med Mol Imaging*. 2019;46:540–557.
20. Lacroix A, Feelders RA, Stratakis CA, Nieman LK. Cushing's syndrome. *Lancet*. 2015;386:913–927.
21. Ziu M, Dunn IF, Hess C, et al. Congress of Neurological Surgeons systematic review and evidence-based guideline on posttreatment follow-up evaluation of patients with nonfunctioning pituitary adenomas. *Neurosurgery*. 2016;79:E541–E543.
22. Castinetti F, Régis J, Dufour H, Brue T. Role of stereotactic radiosurgery in the management of pituitary adenomas. *Nat Rev Endocrinol*. 2010;6:214–223.
23. Govindarajan V, Lu VM, Clarke JE, et al. Positive predictive value and trends of inferior petrosal sinus sampling (IPSS) in diagnosing Cushing disease and ectopic ACTH secretion: a systematic review and meta-analysis. *Clin Neurol Neurosurg*. 2022;220:107350.
24. Wang H, Ba Y, Xing Q, Cai RC. Differential diagnostic value of bilateral inferior petrosal sinus sampling (BIPSS) in ACTH-dependent Cushing syndrome: a systematic review and meta-analysis. *BMC Endocr Disord*. 2020;20:143.
25. Albert NL, Weller M, Suchorska B, et al. Response Assessment in Neuro-Oncology Working Group and European Association for Neuro-Oncology recommendations for the clinical use of PET imaging in gliomas. *Neuro Oncol*. 2016;18:1199–1208.
26. Bergström M, Muhr C, Ericson K, et al. The normal pituitary examined with positron emission tomography and (methyl-<sup>11</sup>C)-L-methionine and (methyl-<sup>11</sup>C)-D-methionine. *Neuroradiology*. 1987;29:221–225.
27. Iglesias P, Cardona J, Díez JJ. The pituitary in nuclear medicine imaging. *Eur J Intern Med*. 2019;68:6–12.
28. Marco Del Pont F, Villalonga JF, Ries-Centeno T, Arakaki N, Katz D, Cervio A. Pituitary adenoma associated with acromegaly and Cushing disease. *World Neurosurg*. 2020;136:78–82.
29. Cenacchi G, Giovenali P, Castrioto C, Giangaspero F. Pituitary adenoma: ultrastructural evidence of a possible origin from folliculo-stellate cells of the adenohypophysis. *Ultrastruct Pathol*. 2001;25:309–312.
30. Sakamoto Y, Takahashi M, Korogi Y, Bussaka H, Ushio Y. Normal and abnormal pituitary glands: gadopentetate dimeglumine-enhanced MR imaging. *Radiology*. 1991;178:441–445.
31. Totani Y, Niinomi M, Takatsuki K, Oiso Y, Tomita A. Effect of metyrapone pretreatment on adrenocorticotropin secretion induced by corticotropin-releasing hormone in normal subjects and patients with Cushing's disease. *J Clin Endocrinol Metab*. 1990;70:798–803.